

Cluster Winds Blow Along Supercluster Axes

Dmitri I. Novikov¹, Adrian L. Melott¹, Brian C. Wilhite¹, Michael Kaufman¹,
 Jack O. Burns², Christopher J. Miller³ and David J. Batuski³

¹Department of Physics and Astronomy, University of Kansas, Lawrence, Kansas 66045, U.S.A.

²Office of Research and Department of Physics and Astronomy, University of Missouri, Columbia, Missouri 65211, U.S.A.

³Department of Physics and Astronomy, University of Maine, Orono, Maine 04469-5709, U.S.A.

2 December 2024

ABSTRACT

Within Abell galaxy clusters containing wide-angle tailed radio sources, there is evidence of a “prevailing wind” which directs the WAT jets. We study the alignment of WAT jets and nearby clusters to test the idea that this wind may be a fossil of drainage along large-scale supercluster axes. We also test this idea with a study of the alignment of WAT jets and supercluster axes. Statistical tests indicate no alignment of WAT jets towards nearest neighbour clusters, but do indicate approximately 98% confidence in alignment alignment with the long axis of the supercluster in which the cluster lies. We find a preferred scale for such superclusters of order 25 Mpc h^{-1} .

Key words: intergalactic medium; cosmology: large scale structure of the universe; galaxies: clusters: general

1 INTRODUCTION

Galaxy clusters are often elongated. Binggeli’s (1982) study of Abell cluster data gave the first indication that they have a strong tendency towards alignment with (i.e., their semi-major axes point toward) other clusters at distances of less than around 30 h^{-1} Mpc. West’s (1989) study of 48 superclusters also gave clear evidence for alignment of clusters within superclusters on similar scales. Simulations also indicate that cluster axes are aligned with neighbouring clusters (Splinter et al. 1997 and references therein).

It has become recognized within the context of structure formation in hierarchical clustering (“bottom-up”) due to gravitational instability that the large-scale weakly non-linear structure closely follows that produced in what used to be called the “top-down” or “pancake” theory (Melott et al. 1983; Pauls & Melott 1995 and references therein; Bond, Kofman, & Pogosyan 1996). In this picture, most galaxy clusters are formed by the flow of matter along the sheets and filaments that connect neighbouring clusters (Shandarin & Klypin 1984, Colberg et al. 1998).

For this reason, merging events are often aligned with these structures. Mergers inject a velocity anisotropy into the cluster that should persist for several crossing times. It may be a cause for the tendency of clusters to point to their neighbours as described above. The anisotropy is a fossil relic of recent merging events, which can be seen most clearly in the simulation video (particularly the second sequence) accompanying Kauffmann & Melott (1992).

Burns (1998) has reviewed the evidence for persistent

winds in the intra-cluster medium that may exist as a result of these recent mergers (see also Gomez et al. 1997a, Roettiger, Burns, & Loken 1996). Gomez et al. (1997b) showed that there was a highly significant correlation between the orientation of the semi-major axis of the cluster and the direction of these winds, as indicated by the bending of jets from wide-angled tailed (WAT) radio sources in the clusters. On the other hand, Ulmer, McMillan, & Kowalski (1989) found no orientation of X-ray images toward nearest neighbour clusters.

Although there is evidence of alignment between cluster ellipticity and neighbour clusters and of alignment of cluster ellipticity with the winds blowing WAT jets, there has been no study of the alignment of WAT jets with neighbour clusters. It is possible that the “prevailing wind” seen in Abell clusters with WATs may be a remnant of drainage along large-scale structure. If this wind is a fossil of such drainage, one might expect that it would point either to neighbour clusters or along supercluster axes.

2 PROCEDURE

Images from Gomez et al. (1997b), Pinkney et al. (1993), Zhao et al. (1989), O’Donoghue, Owen & Eilek (1990), and O’Dea and Owen (1985) are used in the determination of the orientation of wide-angle tailed radio source jets. These images are overlays of 6-cm or 20-cm VLA data on x-ray emission contours in the energy band 0.5–2.0 keV from ROSAT

Cluster	WAT Orientation	Uncertainty
A400	124.3	6.0
A562	320.2	0.2
A690	57.6	2.4
A1446	215.0	7.6
A1569	203.8	2.0
A1656	44.6	3.5
A1940	328.6	1.4
A2214	248.3	9.1
A2304	357.9	4.2
A2306	292.5	1.7
A2462	288.1	1.1
A2634	307.6	2.8

Table 1. Estimated orientation angles for winds in the WAT clusters studied. Note that all angles are taken with respect to the horizontal and are in degrees. Uncertainties represent one standard deviation from estimates by five individuals.

PSPC data. Another image used was of data from the Westbrook radio telescope at 6-cm. (Vallee, Wilson, & VanDerLaan (1979). To estimate the direction of the “wind” within a cluster, lines are drawn manually upon the WAT jets, and a bisector drawn for the angle created by these lines. Since the clusters are all at a large distance from Earth, a small angle approximation is used. The orientation of each bisector in Table 1 is reported with respect to the horizontal. An orientation of 0° or 360° corresponds to a cluster whose WAT “points” to the East on a flattened section of celestial sphere. To reduce the effect of subjectivity upon the estimated orientation of the WATs, lines are constructed independently by five different individuals with no knowledge of the cluster’s environment. As can be seen in Table 1, the random uncertainties in the WAT angle estimation are relatively small and will have little effect on questions of alignment.

We do not consider sources for which orientations were difficult to ascertain for any reason (e.g. extreme ambiguity of orientation; difficulty in determining location of one of the WAT jets; poor spatial radio spatial resolution of the more distant WATs; no apparent wind as evidenced by an opening angle near 180°). We also exclude WATs which live in clusters for which no neighbours exist in our redshift catalog within $30 \text{ Mpc } h^{-1}$, where $h = H_0/100 \text{ km s}^{-1} \text{Mpc}^{-1}$. (This is sometimes due to lack of redshift information.) This leaves us with twelve of the seventeen different WATs that were present in our source studies.

Due to the redshift survey incompleteness, it is not possible to define a complete sample of clusters for the WATs in this analysis. However, given these constraints, we believe that the remaining sample of WAT clusters and their neighbours is not systematically biased and should be representative of such clusters and their environs.

For each of the twelve WATs, we first search the Abell

cluster catalog to find the nearest neighbour cluster. Although all WAT angle bisectors are drawn against a flattened celestial sphere, we find neighbour clusters in three-space. The cluster neighbours of each WAT source are determined using Abell clusters of all richness and distance classes north of -27° declination. In most cases, only clusters with measured redshifts are used. However, approximately 15-20% of Abell clusters with $m_{10} \leq 17.0$ do not as yet have measured redshifts, so occasionally the Batuski & Burns (1985) $m_{10} - z$ relation is used. The data for the clusters with observed redshifts come from a variety of sources including Struble & Rood (1987) and Postman, Huchra & Geller (1992). However, the majority of the cluster redshifts with $m_{10} \geq 16.5$ and $R \geq 1$ were supplied by the MX Survey and its extension (Slinglend et al. 1998; Miller et al.–in preparation). The MX Survey was designed to measure all $R \geq 1$ Abell clusters with $m_{10} \leq 17.0$ in the Northern Hemisphere. Currently, the sample of $R \geq 1$, $0^\circ \leq \alpha \leq 24^\circ$, $-17^\circ \leq \delta \leq 90^\circ$, and $|b| \geq 30^\circ$ Abell clusters is 87% complete to $m_{10} = 17.0$ with 282 out of 324 having measured redshifts. Once the $R = 0$ clusters are included, the sample is 80% complete with 457 out of 569 clusters having measured redshifts. About 90% of the clusters we use have measured redshifts. Two of the nearest neighbours (for A562 and for A2306) have estimated redshifts, but dropping these would not modify our conclusions about nearest neighbours described in the next section. The remaining estimated redshifts are merely a source of foreground/background noise, since we study projected alignments.

All calculations in this paper are made using lines projected upon the celestial sphere and then flattened due to the assumption of a small angle approximation. These calculations should be valid, however, since all these cluster neighbourhoods pictured are relatively small. The largest angular separation between WATs and included clusters is approximately 25° .

Once the nearest neighbour is determined, a line is constructed which connects the WAT cluster to the nearest neighbour. The angle ϕ_i between this line and the WAT bisector is recorded for each of the clusters in Table 2 (index i denotes the number of the WAT). Figure 1 shows the cluster environments and the various orientations we compare. The distribution of these angles is under consideration.

If there is no correlation between the orientations of WATs and directions of the lines connecting WATs and their neighbours, the angle ϕ between them should be uniformly distributed from 0 to 90° and have a mean angle

$$\bar{\phi} = \frac{1}{N} \sum_{i=1}^N \phi_i = 45^\circ, \quad (1)$$

where N is the total number of WATs. If there were any alignment between WAT bisectors and nearest neighbour clusters, then $\bar{\phi}$ would obviously be less than 45° . Equation (1) is accurate for large N , but we have only twelve WATs. $\bar{\phi}$ is 44.4° , and a Kolmogorov-Smirnov test shows no significant evidence that the distribution is non-uniform (see the next section).

We also check for WAT alignment with the supercluster in which the cluster lies. We again search the Abell catalog, this time to locate clusters within $50 \text{ Mpc } h^{-1}$ of each WAT cluster. We loosely call such a set of clusters (including the

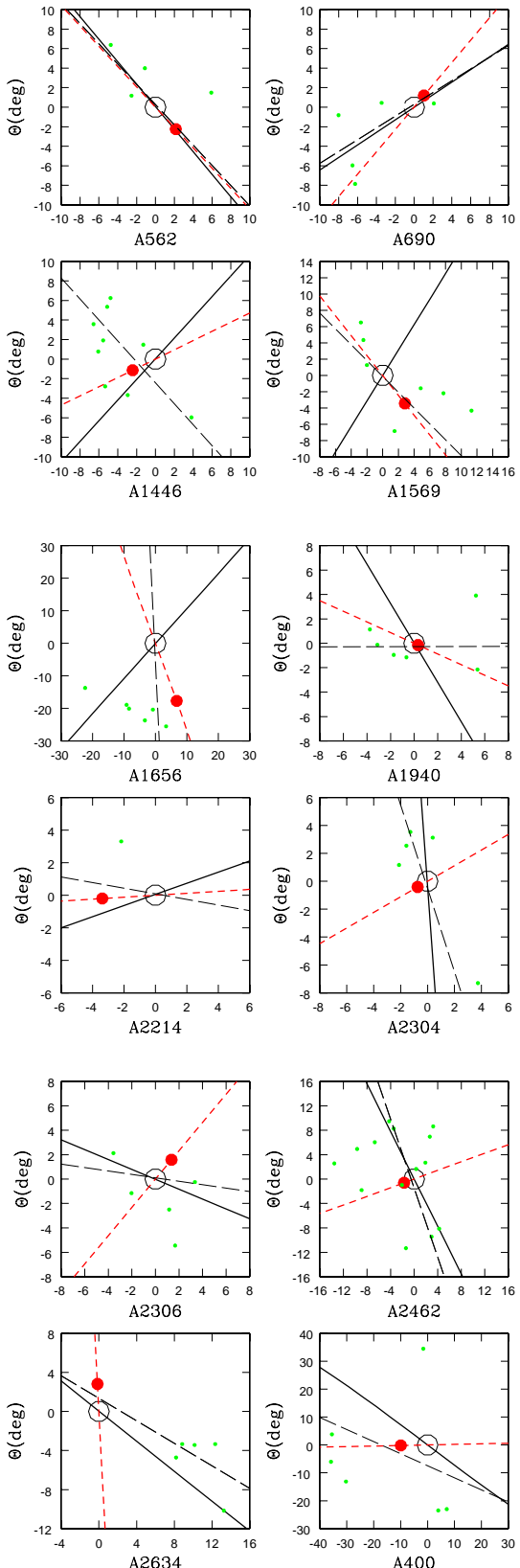


Figure 1. Open circle: WAT cluster; solid line: orientation of the wind blowing the WAT jets; short-dashed line connects WAT cluster with nearest neighbour cluster (large darkened circle); remaining points: clusters within $50 \text{ Mpc } h^{-1}$ of the WAT cluster; long-dashed line: orientation of supercluster as described in text. It must be emphasized that these figures are in projection, while the fit is weighted by full three-dimensional redshift space distances between clusters. Thus the line may not *appear* to be a good fit to the distribution of points.

WAT Cluster	Nearest Neighbour	Angle
A400	A397	36.0
A562	A556	3.3
A690	A699	17.6
A1446	A1402	22.5
A1569	A1526	70.3
A1656	A1367	62.9
A1940	A1936	37.0
A2214	A2213	14.0
A2304	A2304	65.5
A2306	A2305	69.9
A2462	A2459	82.2
A2634	A2666	50.3

Table 2. The nearest neighbour cluster and angle between WAT orientation and a line connecting the WAT and nearest neighbour for each of the clusters studied.

WAT and nearest neighbour clusters) a “supercluster.” We do not include clusters at larger distances from the WAT because this typically forces part of the volume into galactic obscuration or out of the survey region. We have simulated the effect of additional neighbors distributed randomly with the global sample mean density out to $100 \text{ Mpc } h^{-1}$ and find that, while it adds some extra noise, it does not remove our alignment signal.

We next determine the orientation of the supercluster long axis. We wish to fit a straight line to the collection of clusters by drawing a least-squares line based on the projection of each cluster on the flattened celestial sphere. We need to include clusters within a finite distance, to take account of the fact that nearby clusters are more likely to lie within the same structure as the WAT. However, we would like to avoid sudden changes in orientation as this limit is changed to include a new cluster. We therefore apply a least-squares fit to a straight line, but clusters are Gaussian weighted $\exp(-r^2/2r_0^2)$ for proximity to the WAT cluster. An advantage of this approach is that we can explore the effect of changes in r_0 . The angles between the WAT bisectors and these lines are calculated and recorded in Table 3. We have used bootstrap resampling (Barrow, Bhavsar, & Sonoda 1984) to estimate the uncertainty in the angles. For our small number of clusters this procedure is likely to overestimate the uncertainties, so these can be regarded as upper limits to one- σ uncertainties. It is also true that our result does not depend on the assumption that the superclusters are straight lines, while these are the uncertainties in a fit to a straight line. But it is the best we can do to associate some kind of error bars with the orientation of the supercluster. The significance of a correlation between orientation of WAT sources and supercluster axes can be estimated by investigation of the distribution of these angles in the same way as for nearest neighbours.

Figure 1 shows the clusters in the vicinity of the named

WAT Cluster	WAT-Supercluster Angle	Uncertainty
A400	11.0	24.1
A562	3.5	13.2
A690	0.4	8.7
A1446	86.2	7.6
A1569	77.1	10.8
A1656	45.6	7.6
A1940	59.6	8.5
A2214	27.0	23.0
A2304	14.8	14.6
A2306	12.4	25.1
A2462	6.3	12.2
A2634	6.8	7.3

Table 3. The angle between the WAT jet bisector and the line defining the orientation of the supercluster for each of the WAT clusters studied. The supercluster orientation is that for $r_0 = 21 \text{ Mpc } h^{-1}$ (see text).

(WAT-bearing) cluster, along with the orientations of the putative wind (WAT bisector), the direction to the nearest neighbour cluster, and the axis fit as described above. It is important that although actual distances in redshift space are used to decide the weighting, these Figures are seen in projection. Since no radial component of the WAT plasma motion is known, we can only look for correlation in the projected angles. Our weighting is based on three-dimensional distances, but the pictures are in projection, so the orientation line may not *appear* to be a good fit to the positions of the clusters.

3 RESULTS AND DISCUSSION

We perform two Kolmogorov-Smirnov (K-S) tests. The first is done on our distribution of angles between the WAT angle bisector and the line connecting the WAT cluster to its nearest neighbour. This test indicates only a 1.6% confidence level that we may reject the hypothesis of uniform angle distribution. One may ask if cluster wind directions and nearest neighbour directions are correlated with cluster axes, why they are not correlated with one another. It is not required, but we would like a physical explanation. We speculate that cluster axes are affected by both tidal forces and by merger events. One would expect the nearest cluster to dominate the tidal field, but merger events should be correlated with the supercluster axis. Further study is needed to understand this null result.

The second test is on the distribution of angles between the wind (WAT angle bisector) and the supercluster line as defined previously. The angle and therefore the significance of its distribution are obviously functions of r_0 . In Figure 2, the heavy solid line shows the confidence level (for rejection of the null hypothesis that the angles may be distributed

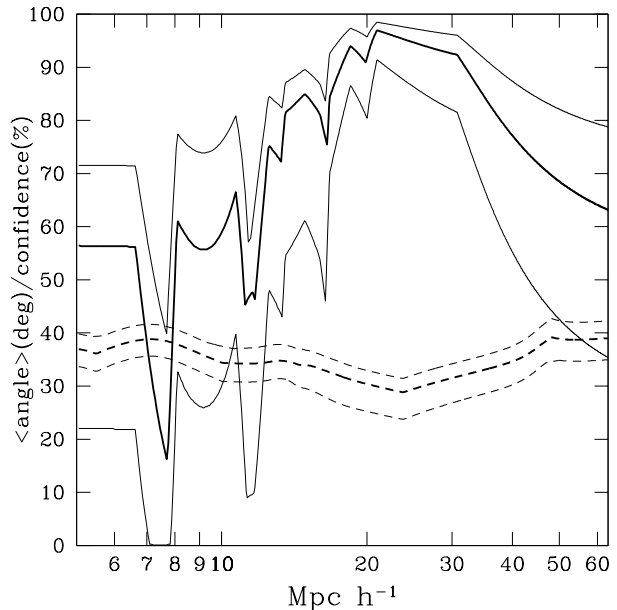


Figure 2. A summary of the results of the supercluster-WAT orientation study. Results are plotted as a function of r_0 , the Gaussian smoothing length for weighting to determine the supercluster orientation. Larger r_0 corresponds to considering a larger neighbourhood of the WAT. The heavy dashed line is the mean angle $\bar{\phi}$ between the wind and the supercluster axis. The lighter dashed lines are the same mean computed using the eleven best and eleven worst alignments. The heavy solid line is the confidence level (as computed by a K-S test) that the distribution of angles in the parent population is not uniform. The light solid lines are the same confidence drawn from the eleven best and worst as described above. It is clear that for superclusters defined in this way, there is a strong tendency for the winds to be aligned with the surrounding region on a scale of about $25 \text{ Mpc } h^{-1}$.

uniformly) as a function of r_0 . This confidence reaches a maximum of 97.0% for $r_0 = 21 \text{ Mpc } h^{-1}$. The lighter solid lines are a measure of the uncertainty in this confidence, generated by choosing eleven best or eleven worst aligned out of the twelve regions. There is clearly a preferred scale, about $25 \text{ Mpc } h^{-1}$. The heavy dashed line is $\bar{\phi}$, which reaches a value of about 29.3° , when the K-S test reaches maximum confidence. (This is not quite the minimum, which is 28.8° .) The mean never exceeds 45° , although the confidence is poor for small and large r_0 . Discontinuities in the slope of the confidence curve occur when the slowly rotating supercluster orientations cross 0° or 90° .

For small r_0 , the supercluster orientation is poorly determined due to the small number of objects included. As r_0 approaches zero, this becomes the nearest neighbour test. For large r_0 , we exceed the scale of typical segments of the network. It is interesting that the region of best r_0 coincides with the wavelength of perturbations going non-linear today as estimated elsewhere (Melott and Shandarin 1993). It is also close to the neighbour linkage radius found necessary for percolation in one supercluster study (Batuski et al. (1998)). We see here support for the idea that the structures found by percolation have a dynamical origin, and are not merely accidental artifacts.

The first K-S test result is consistent with the WAT ori-

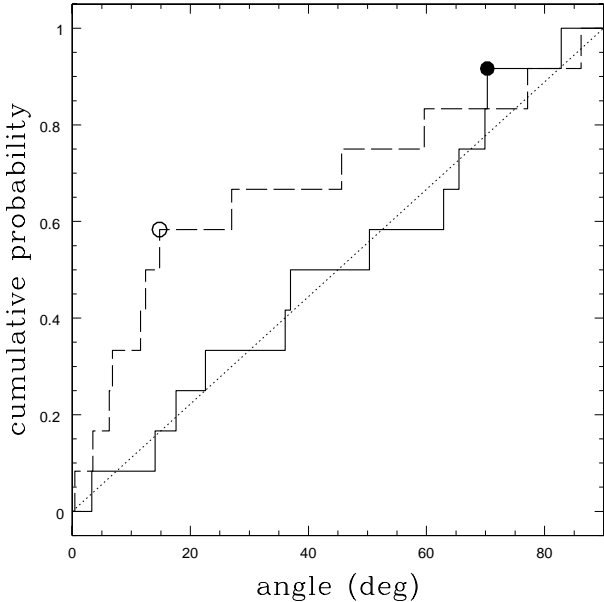


Figure 3. A graphical representation of the Kolmogorov-Smirnov tests performed. The dotted diagonal line represents the expected relationship between angle measures and cumulative probability. The solid stair-step pattern represents this relationship within the nearest-neighbour distribution of angles. The dashed stair-step pattern corresponds to this same relationship for the distribution of supercluster angles. The larger the maximum deviation of the stair-step pattern from the expected diagonal line, the higher the confidence with which one can reject the hypothesis of a uniform distribution of angles. A positive maximum deviation (as seen in both cases here) indicates that the mean angle is less than 45°

entations being completely uncorrelated with nearest neighbours. However, the second K-S test result indicates a strong correlation between WAT wind orientation and the supercluster orientation. It should be noted that a sample size of twelve WAT clusters is very small. West (1989), for example, studied 48 clusters. We recommend investigation of a larger data sample. This will be a lengthy process, dealing with a large number of unclassified sources in the literature.

However, we believe our conclusions on the supercluster-WAT alignment are robust, and offer several reasons for this. First, the K-S test is useful under certain conditions for small sample sizes. It is statistically robust at the sample size and confidence level of our result (Lehmann and D'Abraera 1975).

Another approach is to use a completely different statistic. If we put the angles into four bins of 22.5° , each of which would be equiprobable under a uniform population, we can use the binomial theorem to evaluate the probability that seven or more out of twelve will lie in the first bin. The result is 98.9% confidence that the distribution is not uniform. Using three bins of 30° produces a similar result (98.5%). Apparently the effect we have found is so strong it is significant even for a small sample size.

Our results show a correlation between objects two orders of magnitude apart in size. They are also dynamical evidence in favor of quasi-linear hierarchical clustering following “pancake” dynamics (Melott and Shandarin 1993). This has had great success in reproducing large structure in N-body simulations. It predicted the supercluster-void

picture of large-scale structure accepted today (Zel'dovich, Einasto, & Shandarin 1982, Melott et al. 1983). However, this general agreement between theory and observation has been based on statistical measures of the galaxy distribution, not on observed dynamics. Analysis of cosmic flows has not yet progressed to showing features unique to the quasi-linear regime. The flows indicated here are not a part of linear theory, and thus lend empirical support to the quasi-linear analysis of gravitational instability.

4 ACKNOWLEDGMENTS

We are grateful to the referee, M. West, and also to S. Bhavsar for helpful comments and conversations. DN was supported by an NSF-NATO Fellowship and other authors at the University of Kansas were supported by the NSF-EPSCoR program. JOB was supported by the NSF. CM was funded in part by NASA-EPSCoR program through the Maine Science and Technology Foundation.

REFERENCES

Barrow, J.D., Bhavsar, S.P., Sonoda D.H., 1984, MNRAS, 210, 19P
 Batuski D. J., Burns J. O., 1985, ApJ, 299, 5
 Batuski D.J., Miller C., Slinglend K., Balkowski C., Maurogordato S., Cayatte V., Felenbok P., and Olowin R., 1998 ApJ submitted
 Binggeli B., 1982, A&A, 107, 338
 Bond J.R., Kofman L., Pogosyan D., 1996, Nat, 380, 603
 Burns J.O., 1998, Sci, 280, 400
 Colberg J.M., White S.D.M., Jenkins A., Pearce F.R., MNRAS, submitted (astro-ph/9711040)
 Gomez P.L., Ledlow M.J., Burns J.O., Pinkney J., Hill J.M., 1997a, AJ, 114, 1171
 Gomez P.L., Pinkney J., Burns, J.O., Wang Q., Owen F.N., and Voges W., 1997b, ApJ, 474, 580
 Kauffmann, G.A.M. and Melott, A.L., ApJ, 393, 415 (1992)
 Lehmann E.L. and D'Abraera, H.J.M., 1975, Nonparametrics, (Holden-Day, San Francisco), 38
 Melott A.L., Einasto J., Saar E., Suisalu I., Klypin A., and Shandarin S., 1983, Phys.Rev.Lett, 51, 935
 Melott A.L. and Shandarin S.F., 1993, ApJ, 410, 469
 O'Dea C.P., and Owen F.N., 1985, AJ, 90, 927
 O'Donoghue A., Eilek J., and Owen F.N., 1990 ApJS 72, 75
 Pauls J., Melott A.L., 1995, MNRAS, 274, 99
 Pinkney J., Rhee G., Burns J.O., Hill J.M., Oegerle W., Batuski D., Hintzen, P., 1993, ApJ, 416, 36.
 Postman M., Huchra J. P., Geller M. J., 1992, ApJ, 384, 404
 Roettinger K., Burns J.O., and Loken C., 1996, ApJ, 473, 651
 Shandarin S.F., Klypin A.A., 1984, SvA, 28, 491
 Slinglend K.A., Batuski D.J., Miller C.M., Haase S., Michaud K., Hill J.M., 1998, ApJS, 115, 1
 Splinter R.J., Melott A.L., Linn A.M., Buck C., Tinker J., 1997, ApJ, 479, 632
 Struble M.F., Rood H.J., 1987, ApJS, 63, 543
 Ulmer M.P., McMillan S.L.W., Kowalski M.P., 1989, ApJ, 338, 711
 Vallee J.P., Wilson A.S., VanDerLaan H., 1979 AA, 77, 183
 West M.J., 1989, ApJ, 347, 610
 Zhao J., Burns J.O., and Owen F.N., 1989, AJ, 98, 64.
 Zel'dovich Ya.B., Einasto J., and Shandarin S.F., 1982 Nature, 300, 407

This figure "A2634.jpg" is available in "jpg" format from:

<http://arxiv.org/ps/astro-ph/9808018v2>